Nuclear interferometry and thermal freeze out

David H. Boal and Julian C. Shillcock
Department of Physics, Simon Fraser University, Burnaby, British Columbia, Canada V5A 1S6
(Received 3 September 1985)

The technique of nuclear interferometry is applied to proton and light fragment emission in intermediate energy heavy ion reactions. It is shown that the source radii extracted by the technique are consistently larger for correlations involving two deuterons than for those with two protons. The time scale involved in particle emission is investigated with the technique and places a rough upper bound of a few times 10^{-22} sec on the time scale associated with the source. A cascade model is formulated to predict the source parameters, and these are found to be in at least qualitative agreement with experiment. The implications of these results for the emission of heavier fragments are discussed.

I. INTRODUCTION

There is ample evidence[1] that multiple scattering of nucleons plays an important role in the emission of energetic particles in nuclear reactions,[2] and may lead to a system of particles which is in thermal, and perhaps even chemical equilibrium. In the past, a significant amount of effort has gone into determining how, or even if, such an equilibrated system can be formed. Yet it is equally important to know the time evolution of the system through to when the participants go out of thermal equilibrium.[3] In this paper, attention will be focused on the last stage of the evolution of the nuclear fireball: freeze out.

Several methods, both theoretical and experiment, have already been used to study the thermal history of an intermediate energy reaction (see Ref. 2 for a review). For example, on the theoretical side one can solve the classical diffusion equation, or many other variants, to find the lifetime of the thermalized region in a reaction. Such calculations often indicate lifetimes of less than 10^{-22} sec depending on, among many things, the projectile involved. Alternatively, one can calculate[4,5] the change with time of the chemical abundance of various reaction products, and then use an experimental measurement of these abundances to determine the lifetime. This method also yields lifetimes of less than 10^{-22} sec for those sources which emit energetic ejectiles. Ideally, one would like to have several methods at one's disposal, each of which could measure conditions in the expanding nuclear fireball at a particular density or temperature. This would allow one to map out the temporal evolution of the system. For example, techniques which employ particles with small cross sections may be more sensitive to the early stages of the reaction,[6] whereas particles with larger cross sections would remain in causal contact with the expanding system much longer.[7]

One experimental technique which can make use of this idea is nuclear interferometry:[8] correlations between particles at small relative momenta. Evidence that the cross section effect is important may already have been seen in the different source parameters extracted from two-pion[9] and two-proton[10] interferometry experiments. For light nuclei, such as deuterons and tritons, one would expect to see larger source sizes than are found in two-proton correlations. This was indeed observed[11] in a comparison of dd and tt correlations with pp correlations[12] obtained in ^{16}O-induced reactions on ^{197}Au at $25A$ MeV. One can imagine several effects which may cloud the interpretation of the dd analysis: the large size of the deuteron may not provide sufficient resolving power for the source sizes of interest and the coupled channel nature of the dd interaction also may effect[13] the correlation function. In an effort to resolve these questions we wish to analyze nonidentical particle correlations involving alpha particles: pα and dα. Section II of this paper extends our previous analysis[11] to other data sets[14] and to finite lifetime. The pα and dα results are presented in Sec. III. In Sec. IV, a cascade model will be developed for use in predicting freeze-out parameters, and these will be compared with the data. The implications of this model for the freeze out of heavier composities will also be explored. Section V will contain our conclusions.

II. NUCLEAR INTERFEROMETRY

We will define a correlation function $R(\mathbf{p}_1,\mathbf{p}_2)$ in terms of the inclusive cross section $d^3\sigma/d^3p$ and the coincidence cross section $d^6\sigma/d^3p_1d^3p_2$ via

$$R(\mathbf{p}_1,\mathbf{p}_2)=\sigma_R\frac{d^6\sigma/d^3p_1d^3p_2}{(d^3\sigma/d^3p_1)(d^3\sigma/d^3p_2)}-1\ , \tag{1}$$

where $\mathbf{p}_1$ and $\mathbf{p}_2$ are the momenta of particles 1 and 2. In experimental practice, σ_R is taken to be a normalization constant chosen so that $R\rightarrow 0$ when the relative momentum, $\Delta p=\mu\,|\,\mathbf{p}_1/m_1-\mathbf{p}_2/m_2\,|$ becomes large.

One approach to predicting the behavior of R will be to follow the approach[8] used in $\pi\pi$ and pp analysis that the particles are emitted independently from a source which is assigned some functional form in space and time. We will follow the convention first used for noncomposite parti-

cles and parametrize the source region as a Gaussian in space and time, with parameters r_0 and τ. The assumption of a Gaussian time dependence rather than the more usual exponential decay arises because we consider the emission of particles from the source region to be statistically independent. The source thus acts as an ensemble of independent emitters rather than as a decaying excited state. One could alternatively describe the correlations in a thermal model approach where the presence of resonances perturbs the density of states of the two particle system, but the results would be equivalent.[15]

For two-deuteron correlations, one can then write

$$1+R(\mathbf{p}_1,\mathbf{p}_2)=\frac{1}{(2\pi)^{3/2}r_0^2\rho}\int d^3r \exp\{-[r^2-(\mathbf{r}\cdot\mathbf{v}'\tau/\rho)^2]/2r_0^2\}[\tfrac{1}{9}|{}^1\psi_{\Delta p}(\mathbf{r})|^2+\tfrac{1}{3}|{}^3\psi_{\Delta p}(\mathbf{r})|^2+\tfrac{5}{9}|{}^5\psi_{\Delta p}(r)|^2], \quad (2)$$

where $\rho^2=r_0^2+(v'\tau)^2$. In this expression, $\mathbf{v}'=\mathbf{v}-\mathbf{v}_0$ where $\mathbf{v}$ is the velocity of the two-particle center of mass and $\mathbf{v}_0$ is the velocity of the emitting region. The superscript on the dd wave functions is equal to $2s+1$, s being the spin of the pair. Equation (2) involves both a radial and an angular integral, the latter being done analytically by expanding the exponential as a power series in $\mathbf{r}\cdot\mathbf{v}'\tau$. Because this procedure has convergence problems at $v'\tau > r_0$, it will be assumed for the time being that $\tau=0$.

The wave functions were treated as follows: A partial wave expansion was used, the angular part being integrated analytically. The radial wave functions were obtained by numerically integrating the Schrödinger equation with both Coulomb and nuclear potentials for low orbital angular momenta ($l \leq 2$); for larger orbital angular momenta the nuclear part was neglected. The resulting wave functions were normalized to spherical Coulomb waves at large radii where the nuclear potential is negligible. The Coulomb waves were generated by means of the recurrence relation

$$l[(l+1)^2+\eta^2]^{1/2}F_{l+1}=(2l+1)\left[\eta+\frac{l(l+1)}{\rho}\right]F_l - (l+1)[l^2+\eta^2]^{1/2}F_{l-1}, \quad (3)$$

where η is the Sommerfeld parameter and F_l is a solution of the Schrödinger equation

$$F_l''(\rho)+\left[1-\frac{l(l+1)}{\rho^2}-\frac{2\eta}{\rho}\right]F_l(\rho)=0. \quad (4)$$

The primes denote differentiation with respect to $\rho=kr$, the wave vector of the relative motion being k. For $\tau=0$, the sum over partial waves was extended to $l=15$ for small relative momenta and increased stepwise up to $l=80$ for large relative momenta. The radial integration was taken out to 100 fm. For $\tau\neq 0$, l was truncated at 12. We believe the numerical accuracy of the calculated correlation function to be better than 4%.

For each partial wave, the nuclear potential was parametrized in terms of a Woods-Saxon potential. For dd scattering, we will make use of two sets of potential parameters R, a, and V_0 which were obtained in Ref. 11 by fitting the energy dependent phase shifts extracted from dd scattering. The most complete set of phase shifts in the energy range required for these calculations was obtained by application of the coupled channel R-matrix (RM) approach[16] and led to predominantly repulsive potentials [labeled a in Fig. 1]. The other set of phase shifts was obtained by the resonating group (RG) approach,[17] b, from data at a higher energy than is required here. A table of the potential parameters is given in Ref. 11.

The predictions of these calculations (as well as one in which the nuclear terms were dropped) are contrasted in Fig. 1 with the data[14] from the 400A MeV Ca + Ca reaction. No attempt has been made in these predictions to account for the angular size of the detectors, etc. As was found with the 25A MeV experiment, the RM phase shift set is favored over the RG one. Further, the source parameter r_0 is seen to have a value in the 6 fm range, again as was found in the low energy data. This value for r_0 is about 50% larger than that found in the analysis of the two-proton correlation function. Further, if one equates the rms radius of this Gaussian distribution with that of a uniform density distribution of radius R_u, then it is clear that the density of the deuteron source must be very low, since $R_u=\sqrt{5/2}r_0$.

The two-triton data indicate similarly large source

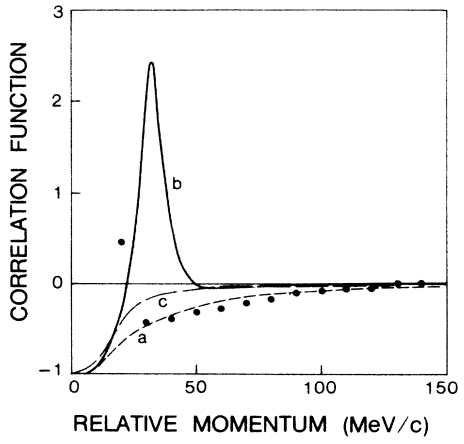

FIG. 1. Two-deuteron correlation function measured (Ref. 14) for 400A MeV Ca + Ca. The theoretical curves show the results for several different sets of phase shifts: R-matrix, a, and resonating group, b, results for the nuclear parts of the dd phase shifts as well as pure Coulomb, c. The parameter r_0 was taken to be 6 fm. The error bars on the data have been omitted, but are substantial for small relative momenta.

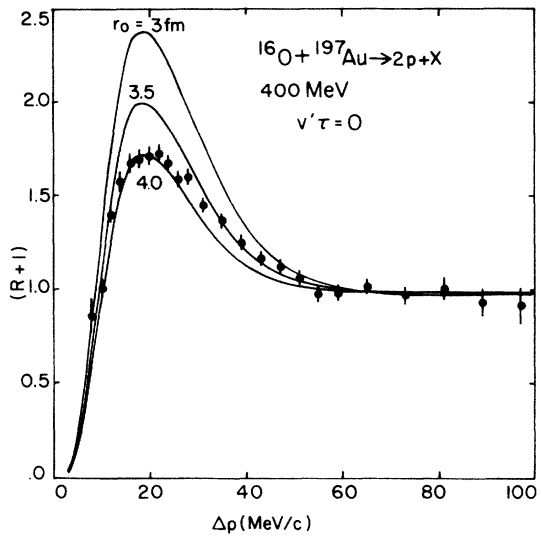

FIG. 2. Two-proton correlation functions measured (Ref. 12) in a 25A MeV $^{16}O + Au$ reaction. Theoretical curves for several different Gaussian source parameters are shown for comparison.

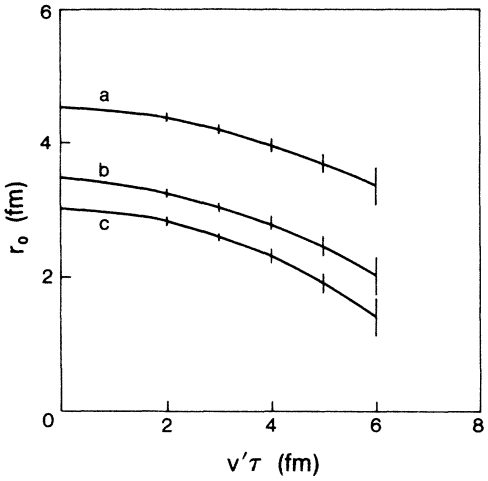

FIG. 3. Loci of values of $(r_0, v'\tau)$ which reproduce the peak height of the pp correlation function data (Ref. 12) at 25A MeV. The curve labels refer to the summed proton energy cuts used in analyzing the data: $E_1+E_2=60$ MeV, a; 80 MeV, b; and 100 MeV, c.

sizes. Unfortunately, we have not been able to perform a complete calculation due to the limited data on low energy triton-triton scattering. However, the prediction for Coulomb wave functions alone is not too different from the low energy data (the statistics of the 400A MeV tt data at small Δp preclude comparison) indicating that the source must be sufficiently large that the nuclear part of the tt interaction does not play a dominant role.

The above results are for $\tau=0$. If τ is now allowed to be finite then one would expect that the value of r_0 associated with such a τ which would reproduce the data, would be smaller than that found for $\tau=0$. For example, we have performed a calculation for the pp measurements at 25A MeV in which a locus of values of $(r_0, v'\tau)$ was obtained which reproduced the peak in the correlation function at $\Delta p \sim 20$ MeV/c. An example of the pp correlation function is shown in Fig. 2. When energy cuts were made on the proton energies, it was found that the peak height increased with proton energy, perhaps indicating a smaller source. In Fig. 3 we show the $(r_0, v'\tau)$ curves for several values of the summed proton kinetic energies. One can see that r_0 decreases slowly for increasing $v'\tau$. However, it is difficult to imagine that r_0 would have a value more than 50% below the $\tau=0$ value, since an unrealistically large source density would be required. Taking $v'\tau=6$ fm in Fig. 3, and assuming that the source velocity is half of the beam velocity, one can estimate τ. At the detector angle of 15° this would then correspond to $\tau=1.4\times10^{-22}$, 1.1×10^{-22}, and 0.9×10^{-22} sec for curves a, b, and c, respectively. These time scales are in the range which is expected from the arguments presented in the Introduction. The ingredients of the pp calculation performed here follow very closely those described in Ref. 8. Similar results were found for the dd correlation function: r_0 changed by less than 10% as τ was increased from 0 to 7×10^{-23} sec (corresponding to $v'\tau$ of 2.5 fm).

As $v'\tau$ approaches r_0, ever more terms in $(v'\tau/\rho)^2$ must be kept in the expansion of the exponential in the integral in Eq. (2). Beyond $v'\tau=6$ fm in Fig. 3, the numerical integrations used in the calculation [which involved keeping terms up to $(v'\tau/\rho)^{20}$] became overly long, and we have not pursued this approach further. An alternate approach, which can be used to provide an upper bound on $v'\tau$, is to take the $r_0\to0$ limit of the Gaussian. The correlation function then has the convenient form (for two-proton correlations)

$$R(\mathbf{p}_1,\mathbf{p}_2)=\frac{4}{(2\pi)^{1/2}v'\tau}\int_0^\infty dZ\, e^{-Z^2/2(v'\tau)^2}\left[\frac{1}{4}\left|\sum_{l_{\text{even}}}\Phi_l(kZ)P_l(\cos\theta')\right|^2+\frac{3}{4}\left|\sum_{l_{\text{odd}}}\Phi_l(kZ)P_l(\cos\theta')\right|^2\right], \tag{5}$$

where θ' is the angle between $\mathbf{v}'$ and $\Delta\mathbf{p}$ and Φ_l is the radial part of the lth partial wave.

To make use of Eq. (5), one needs to know the angle between Δp and v', a quantity which is often experimentally averaged over. Because of this limitation on its use, we will apply the $r_0\to0$ approach only to dd correlations. For deuterons with an average energy of 40 MeV and a source velocity of half of the beam velocity, we find that τ must be 2×10^{-22} sec to reproduce the $r_0=6$ fm calculation for $\Delta\mathbf{p}$ and $\mathbf{v}'$ parallel. For $\Delta\mathbf{p}$ not parallel to $\mathbf{v}'$, the value of τ can be much larger. Since a delta function source is an unlikely approximation to the real source for

deuteron emission, this upper bound on τ is probably not particularly useful.

III. NONIDENTICAL PARTICLE CORRELATIONS

Since there are obviously fewer like-particle pairwise combinations available than there are unlike combinations, to obtain more experimental information one will have to be less restrictive than examining only like-particle correlations. In particular, because of the interpretational questions raised in the Introduction about dd correlations, there is an advantage to using α particles in the correlation measurements. This allows one to have a probe with a larger cross section than a nucleon, yet still be compact and sufficiently tightly bound to avoid the coupled channel problem in some cases. Of course, since the α particle has zero spin, some other difficulties encountered with dd are also avoided.

Once the identical particle assumption is dropped, the breakup of the partial wave sums into even and odd series no longer applies. However, the calculations are no more complicated and we follow the same methods as before.

As input to the correlation function calculation, low energy wave functions for the two-particle system are needed. We proceed by analyzing nuclear phase shift data with a Woods-Saxon potential. The charge is assumed to be distributed uniformly within a radius of 3.0 fm. The results for fitting the s and p waves of the $p+\alpha$ system are shown in Table I. It has been assumed that the s-wave phase shift begins with a value between $\pi/2$ and π at zero energy (as in Refs. 18 and 19), rather than decreasing from 0 and being negative over the range of energies considered here. A comparison of the experimental phase shifts with those corresponding to Table I are shown in Fig. 4. The difference between the calculated and experimental $^2P_{1/2}$ phase shift is only important for laboratory energies greater than 10 MeV, which corresponds to relative momenta greater than 110 MeV/c. It is thus negligible in the region of interest. These potential parameters are then used to predict the pα correlation function shown in Fig. 5. The prominent peak in the predicted correlation function and the data[20] corresponds to the ^{5}Li ground state in the $J=\frac{3}{2}$ wave. As with the dd results, one can

TABLE I. Woods-Saxon potential parameters obtained in our analysis of the $p+\alpha$ phase shift data of Refs. 18 and 19. All potentials are attractive.

l	j	V_0 (MeV)	R (fm)	a (fm)
0	$\frac{1}{2}$	−25.575	3.050	0.938
1	$\frac{1}{2}$	−27.269	2.231	0.682
1	$\frac{3}{2}$	−30.929	2.700	0.488
2	$\frac{3}{2}$	−4.0	1.5	1.0
2	$\frac{5}{2}$	−3.4	2.0	1.0

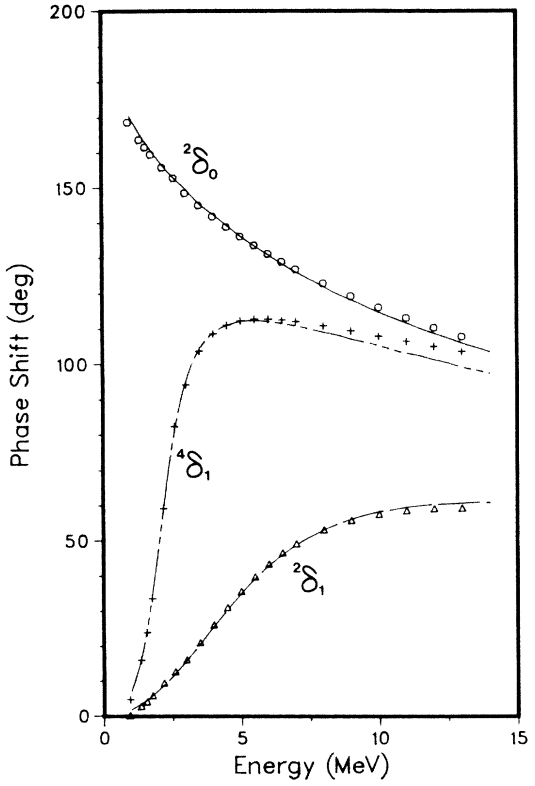

FIG. 4. Comparison of experimentally determined $p+\alpha$ phase shifts (Refs. 18 and 19) with those corresponding to the potential parameters of Table I.

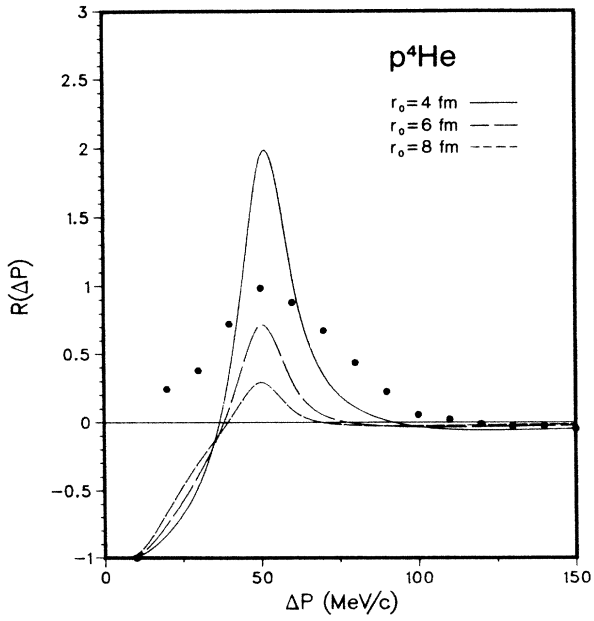

FIG. 5. Predicted pα correlation functions for various values of the source parameter r_0. The data (Ref. 20) are from 400A MeV Ca + Ca.

see that a value for r_0 in the 6 fm range is required to fit the data. The disagreement between theory and experiment is probably attributable in large part to our neglect of the smearing of the correlation function arising from detector geometry, resolution, etc. For systems where we have been able to take these factors into account (see the $d\alpha$ results below, as well as Ref. 21) the agreement is considerably better.

The $d + \alpha$ phase shifts are more involved. Because of the sensitivity of the d-wave resonance (^{6}Li excited state at 2.19 MeV above the ground state) to the numerical techniques used to generate the phase shifts, we decided to refit the phase shift data rather than use the optical model analysis of Ref. 22. The charge is assumed to be distributed uniformly within a relative radius of 4.0 fm. The Woods-Saxon potential parameters so obtained are shown in Table II. The quality of the fit to the data is similar to that shown for the $p + \alpha$ example. The 2.19 MeV excited state is very narrow, and its width is exceedingly sensitive to small changes in the potential parameters chosen. However, because the experimental resolution of the measured correlation function is much wider than the resonance, this did not result in the predicted correlation function being overly sensitive to the parameters. The predictions are shown in Fig. 6. One sees in both the data[23] and the calculation a very large correlation at the 2.19 MeV state. Because the predicted correlation is so sharp, what is shown in the figure is the calculated value smeared out by the resolution function used in Ref. 23. For both of the peaks in the correlation function, a value for r_0 of 6 fm is required to reproduce the data. However, some caution should also be exercised in comparing the results from the different data sets because of the different projectile/target masses. Thus, the 25A MeV data (^{16}O on ^{197}Au) should show smaller dimensions than the 60A MeV results (^{40}Ar + ^{197}Au). Clearly, nonidentical particle correlations will be able to provide a wealth of information about source evolution. We have not been able to make predictions for all fragment combinations which should be accessible experimentally; however, for completeness sake we have compiled results for correlation functions using Coulomb wave functions only in Fig. 7.

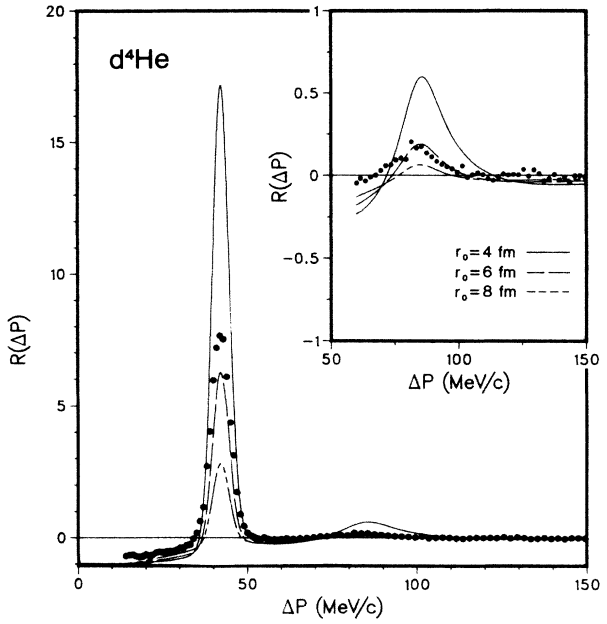

FIG. 6. Predicted $d\alpha$ correlation functions for various values of the source parameter r_0. The data (Ref. 23) are from 60A MeV Ar + Au. Because the prominent peak at $\Delta p \sim 40$ MeV/c is so sharp, we have used the experimental resolution function from Ref. 23 to smear out the calculated correlation function. A more detailed view of the correlation function around the region of the second peak at ~ 80 MeV/c is shown in the inset.

IV. A MODEL FOR FREEZE OUT

In energetic heavy ion reactions, it may be possible to imagine the expansion and cooling of the energetic particle emission region without concerning oneself about its interaction with the other blobs of cold matter. Let us construct a model for the expansion phase.[24] It will be assumed that by the time the initial thermalization step of the reaction is over, the hot fireball which is produced has no large scale inhomogeneities and has a density of about nuclear matter. As the system evolves, both the initial temperature T_0 which characterizes the system and the density ρ will decrease. It will be assumed, therefore, that in the expansion phase three-body interactions can be neglected, an assumption which improves as freeze out is approached. For convenience, the participant nucleons will be uniformly distributed in a spherical volume. The time evolution of this system is then followed in the cascade model sense: a Monte Carlo initialization of the system is made and then the trajectories of the nucleons are computed using relativistic mechanics but ignoring quantum effects. Typically 200 or more such events are averaged over to obtain reasonable statistics.

TABLE II. Woods-Saxon potential parameters obtained in our analysis of the $d + \alpha$ phase shift data of Ref. 22. A negative sign indicates an attractive potential.

l	j	V_0 (MeV)	R (fm)	a (fm)
0	1	−5.82	3.8767	0.1963
1	0	0.3586	5.57	0.55
1	1	0.749	4.14	0.566
1	2	1.147	3.848	0.551
2	1	−11.3646	4.1823	0.4712
2	2	−31.0	2.916	0.6386
2	3	−42.045	2.7648	0.70

To compare the results of this model with experiment, we first estimate the freeze-out density by finding the elapsed time at which the average reaction time τ_{reac} exceeds the expansion time, τ_{exp}, of the system. The reaction time is obtained simply by counting the number of NN collisions in a particular time bin. The characteristic expansion time of the system is defined here by

$$\tau_{\text{exp}} = \langle r^2 \rangle^{1/2} / (d\langle r^2 \rangle^{1/2}/dt) \, . \tag{6}$$

In this model, the nucleons are assumed to obey Maxwell-Boltzmann statistics and Pauli blocking is omit-

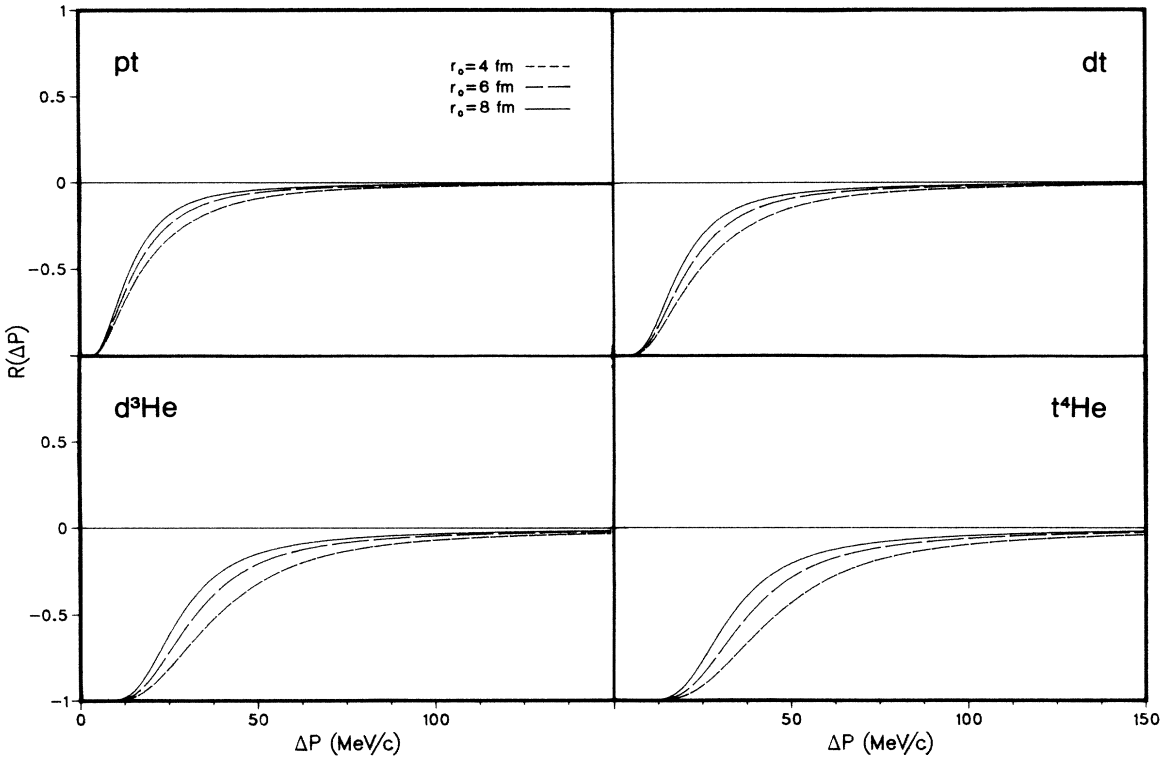

FIG. 7. Correlation function predicted for several nonidentical particle correlations using Coulomb wave functions only.

ted so the model will not be applicable to low energy reactions. The effective nucleon-nucleon cross section is taken to be 30 mb. Decreasing this value will decrease the calculated source radii.

One can use the rms radius obtained at freeze out to make a comparison with the two-particle correlation results, as is shown in Fig. 8. The experimental data[14] are from Ca + Ca collisions at 400 A MeV, and the source parameter is shown as a function of charged particle multiplicity. For the theoretical curve, it has been assumed that the number of nucleons in the source is double the charged particle multiplicity, and that the initial distribution has a temperature of 40 MeV. The value of r_0 obtained from the model is that of a Gaussian distribution

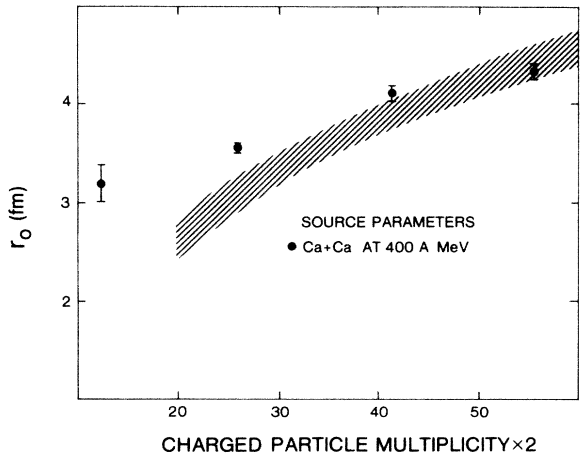

FIG. 8. Comparison of source parameter r_0 obtained in 400 A MeV Ca + Ca collisions with the model calculation. For simplicity, it has been assumed that the total multiplicity is double the charged particle multiplicity obtained experimentally. The experimental results are obtained by an analysis in which the source lifetime is put equal to zero, while the model has a finite source lifetime.

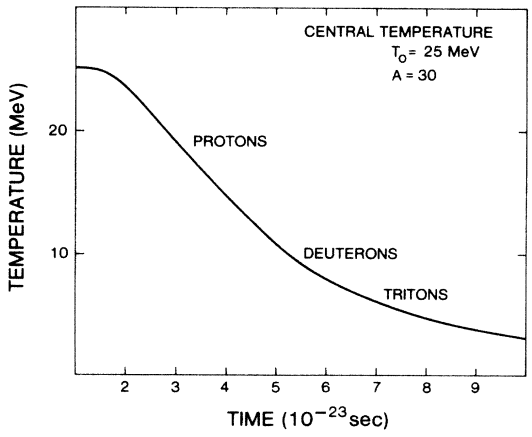

FIG. 9. Model calculation of the temperature in the region $r \lesssim 2$ fm for a 30 nucleon system shown as a function of time. The estimated freeze-out times are indicated for several particle species.

with the same rms radius as that found numerically: $r_0=\sqrt{2/3}r_{\rm rms}$. One can see that the agreement is at least qualitative. If one corrects for the finite lifetime of the source ($\tau=0$ for the data analysis shown in Fig. 8) then r_0 obtained experimentally, will decrease. It is difficult to assign a freeze-out density in this calculation because the density is not uniform. However, an average value would be about $\frac{1}{2}$ nuclear matter density.

One can estimate the freeze-out densities for deuterons and tritons in a similar fashion. Again, because of the neglect of Pauli blocking, the model will only be applied to the high energy data. The initial temperature is taken to be 40 MeV and the source is assumed to have 40 nucleons. The nucleon-nucleus cross section is parametrized as $2\pi A^{2/3}$ fm^2 from a comparison with neutron-nucleus scattering data.[25] The model shows an increase in the value of r_0 (5 fm for deuterons, 6–7 fm for tritons) over the proton results of about 50% for these nuclei, as is found experimentally. The kinetic freeze-out density for deuterons is roughly $\frac{1}{4}$ nuclear matter density.

As the system expands, the temperature (as measured in a comoving frame) decreases. Shown in Fig. 9 is the behavior of the temperature in the central region ($r\leq 2$ fm) of the fireball as a function of time. The approximate kinetic freeze-out times for several species are indicated. This decrease in the local temperature does not necessarily imply a shift in the energy spectrum. For example, if we started with a fixed number of particles forming an ideal gas, then conservation of energy would imply that the average energy per particle remain constant. What should change, however, is the relative abundance of particle species. So long as a species remains in chemical equilibrium, its abundance relative to other species will be determined by the local temperature. Hence, excited state populations, or the abundance of certain nuclei which are less well bound than others, should decrease with increasing time until freeze out of the species involved. In addition to using two particle correlations, then, to determine freeze-out parameters, one could also use the chemical abundances of various nuclear species.

For example, the moving source model fits[26] to intermediate rapidity fragment emission in heavy ion reactions in the $100A$ MeV range show temperatures in the 25–30 MeV region. One can use the integrated light fragment yields to obtain an estimate of the chemical temperatures. The technique should work best for a sequence of isotopes, since any complications introduced by Coulomb effects should be comparable in each isotope. A model in which there is a chemical equilibrium among fragment species is assumed, so that data on at least three isotopes is required in order to eliminate the free parameters. We find for the Ar + Ca and Ar + Au data at $137A$ MeV that the Li, Be, and B isotopes show chemical temperatures in the 2–3 MeV range, about a factor of 10 lower than the kinetic temperatures.[27] Unfortunately, the statistical accuracy of the data limited our ability to extend the technique to sequences of isotones and isobars. This magnitude of decrease is quantitatively what one expects from the cascade model for expansion described here. The recently reported excited state population measurements[23,28] may also be examples of this effect.[7]

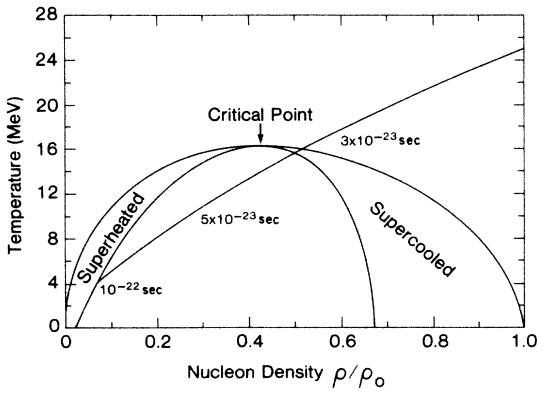

FIG. 10. Liquid-gas phase transition region (from Ref. 29) and an estimated reaction path for a system with an initial temperature of 25 MeV. The particles obey Maxwell-Boltzmann statistics in these calculations. The elapsed time during the expansion phase is also indicated.

To summarize, the cascade model presented here can be used to obtain source dimensions as well as freeze-out densities and temperatures. The predictions agree at least qualitatively with the existing two-particle correlation data, as well as freeze-out temperatures obtained from population ratio arguments. An immediate application of this model can be found in the study of the liquid-gas phase transition boundaries as given in Ref. 29. The cascade approach can then be used to find the reaction trajectory in the phase transition region. Shown in Fig. 10 is the trajectory of the central region in an expanding gas of Maxwell-Boltzmann nucleons, starting at a temperature of 25 MeV and normal nuclear matter density. One can see that the trajectory takes one into the phase transition domain. Whether the system (or some components of it) is actually in equilibrium by the time the transition region is reached depends on the species being examined. But it is clear from Fig. 9 that light mass fragments are probably still in equilibrium when the mechanical instability region is reached.

V. CONCLUSION

It has been shown that the linear dimension of the emitting region for deuterons is about 50% larger than is found for protons in an analysis of two-particle correlation measurements in heavy ion reactions. Nonidentical particle correlation functions involving α particles were also analyzed and shown to give similarly large values for the source dimension. An attempt was also made to estimate the time scale involved. For nucleon emission, time scales much longer than 10^{-22} sec probably require unrealistically small values of r_0 to reproduce the data. It was not found to be possible to obtain an accurate value for the time, although use of a δ-function source for the spatial region allowed a rough upper bound of 3×10^{-22} sec to be placed on τ for deuteron emission. The increasing source radii suggest that there may be a sequential freeze out of various nuclear species, nuclei with larger cross sections going out of equilibrium later than those

with smaller cross sections. A cascade model was presented which allowed an estimate of the freeze-out densities and temperatures to be made for light nuclei in the low density regimes and these estimates were shown to be consistent with the experimental results.

This model was then used to find the trajectory of the expansion regime in the T,ρ plane, in particular to see in what part of the phase transition regime it lay. The calculations show that light and medium mass fragments probably go out of equilibrium near the phase transition region for heavy ion reactions. However, it is not clear whether the phase transition will significantly modify the cluster size distribution built up as the system moves toward the transition region.

ACKNOWLEDGMENTS

We would like to thank E. D. Cooper and B. Jennings at TRIUMF for several helpful discussions. The authors also thank C. K. Gelbke, B. Jacak, and H. Wieman for providing data prior to publication. This work was supported in part by the Natural Sciences and Engineering Research Council of Canada.

[1]For a review of the thermal model, see S. Das Gupta and A. Z. Mekjian, Phys. Rep. **72**, 131 (1981).

[2]For a review of energetic particle emission, see, D. H. Boal, in *Advances in Nuclear Physics,* edited by J. W. Negele and E. Vogt (Plenum, New York, 1985), Vol. 15.

[3]For several different approaches to this problem, see, for example, H. Stöcker, J. Hofmann, J. A. Maruhn, and W. Greiner, Prog. Part. Nucl. Phys. **4**, 133 (1980); N. Stelte and R. Weiner, University of Marburg Report, 1984.

[4]D. H. Boal, Phys. Rev. C **29**, 967 (1984).

[5]A. Z. Mekjian, Nucl. Phys. **A384**, 492 (1982).

[6]S. Nagamiya, Phys. Rev. Lett. **49**, 1383 (1982).

[7]D. H. Boal, Phys. Rev. C **30**, 749 (1984).

[8]For applications in nuclear physics, see S. E. Koonin, Phys. Lett. **70B**, 43 (1977); F. B. Yano and S. E. Koonin, *ibid.* **78B**, 556 (1978).

[9]W. A. Zajc *et al.*, Phys. Rev. C **29**, 2173 (1984); see also D. Beavis *et al.*, *ibid.* **28**, 2561 (1983).

[10]F. Zarbakhsh *et al.*, Phys. Rev. Lett. **46**, 1268 (1981).

[11]C. B. Chitwood *et al.*, Phys. Rev. Lett. **54**, 302 (1985).

[12]W. G. Lynch *et al.*, Phys. Rev. Lett. **51**, 1850 (1983).

[13]P. J. Siemens, private communication.

[14]H. A. Gustafsson *et al.*, Phys. Rev. Lett. **53**, 544 (1984); and private communication.

[15]B. K. Jennings, D. H. Boal, and J. C. Shillcock, submitted to Phys. Rev. C.

[16]G. M. Hale and B. C. Dodder, in *Few-Body Problems in Physics,* edited by B. Zeitnitz (Elsevier, Amsterdam, 1984), Vol. II.

[17]F. S. Chwieroth *et al.*, Nucl. Phys. **A189**, 1 (1972).

[18]A. L. Brown, W. Haeberli, and W. Trächslin, Nucl. Phys. **A90**, 339 (1967).

[19]P. Schwandt, T. B. Clegg, and W. Haeberli, Nucl. Phys. **A163**, 432 (1971).

[20]H. A. Gustafsson *et al.*, private communication.

[21]C. B. Chitwood *et al.* (unpublished).

[22]L. C. McIntyre and W. Haeberli, Nucl. Phys. **A91**, 382 (1967).

[23]J. Pochodzalla *et al.*, Phys. Rev. Lett. **55**, 177 (1985).

[24]For a discussion of the role of fireball expansion during particle emission, see S. E. Pratt, Phys. Rev. Lett. **53**, 1219 (1984).

[25]For a summary, see V. A. Nedzel, Phys. Rev. **94**, 174 (1954).

[26]B. V. Jacak, private communication.

[27]A similar effect has previously been noted in proton induced reactions. See A. S. Hirsch *et al.*, Phys. Rev. C **29**, 808 (1984) and references therein.

[28]D. J. Morrissey, W. Benenson, E. Kashy, B. Sherrill, A. D. Panagiotou, R. A. Blue, R. M. Ronningen, J. van der Plicht, and H. Utsonomiya, Phys. Lett. **148B**, 423 (1984).

[29]A. L. Goodman, J. I. Kapusta, and A. Z. Mekjian, Phys. Rev. C **30**, 851 (1984).